Noncontact orientation of objects in three-dimensional space using magnetic levitation

Anand Bala Subramaniam[a], Dian Yang[b], Hai-Dong Yu[a], Alex Nemiroski[a], Simon Tricard[a], Audrey K. Ellerbee[a], Siowling Soh[a], and George M. Whitesides[a,c,d,1]

[a]Department of Chemistry and Chemical Biology, [b]School of Engineering and Applied Science, [c]Wyss Institute for Biologically Inspired Engineering, and [d]The Kavli Institute for Bionano Science, Harvard University, Cambridge, MA 02138

This paper describes several noncontact methods of orienting objects in 3D space using Magnetic Levitation (MagLev). The methods use two permanent magnets arranged coaxially with like poles facing and a container containing a paramagnetic liquid in which the objects are suspended. Absent external forcing, objects levitating in the device adopt predictable static orientations; the orientation depends on the shape and distribution of mass within the objects. The orientation of objects of uniform density in the MagLev device shows a sharp geometry-dependent transition: an analytical theory rationalizes this transition and predicts the orientation of objects in the MagLev device. Manipulation of the orientation of the levitating objects in space is achieved in two ways: (*i*) by rotating and/or translating the MagLev device while the objects are suspended in the paramagnetic solution between the magnets; (*ii*) by moving a small external magnet close to the levitating objects while keeping the device stationary. Unlike mechanical agitation or robotic selection, orienting using MagLev is possible for objects having a range of different physical characteristics (e.g., different shapes, sizes, and mechanical properties from hard polymers to gels and fluids). MagLev thus has the potential to be useful for sorting and positioning components in 3D space, orienting objects for assembly, constructing noncontact devices, and assembling objects composed of soft materials such as hydrogels, elastomers, and jammed granular media.

magneto-Archimedes levitation | self-assembly | soft robot | colloidosomes | equilibrium

Developing new techniques to manipulate and orient components is part of the developing field of advanced manufacturing. Procedures for orienting hard objects reliably in three dimensions (3D) are essential for many existing manufacturing processes and relevant to a range of applications in other areas (1). Examples include operating automated manufacturing lines, sorting and prepositioning components for assembly, and inspecting parts for quality control. Components in assembly lines often have random orientations, and they must be oriented properly before assembly (2–4). Advanced and "next-generation" approaches based on biomimetic (5–8) and soft robotic (9) strategies, and hierarchically organized, self-assembled, and stimulus-responsive materials (10–15) particularly require methods capable of orienting and assembling soft, sticky, and easily damaged materials. Few methods exist to manipulate these types of materials without damaging them.

One way of orienting hard objects is to agitate them mechanically, and to allow them to fit (or fall) into openings of complementary shape (2); for appropriate geometries, a correct fit ensures that the object is appropriately oriented and can be transported to the next process. The disadvantages of this method are that it can be slow, and that it is not suitable for objects that are soft, fragile, or sticky. Most importantly, it is only reliable for objects of anisotropic shape: that is, it fails for objects that have only slightly asymmetrical shapes or sizes (16, 17).

Robotics provides an alternative method for orienting hard objects. Robotic arms can grasp and arbitrarily position objects that are randomly oriented, but to do so, they require imaging devices, sensors, and complex control algorithms (3). Such robots,

therefore, must incorporate complex, expensive vision systems (18); such systems also do not work well with soft materials (19, 20) [although soft robots (21, 22) and grippers (23) may develop to a level at which they ease the task of manipulating soft or fragile objects]. In general, automated systems (e.g., "pick-and-place" robotic systems) handle objects of specific shapes, and are not designed for general-purpose recognition and manipulation of objects of arbitrary shapes and materials (24, 25). Thus, changes in a manufacturing process may require extensive modifications to a robotic system before it can handle objects of (even slightly) different shapes or sizes (26).

This paper describes several noncontact methods of orienting both hard and soft objects of different shapes and sizes using Magnetic Levitation (MagLev). Objects are suspended in aqueous solutions of a paramagnetic salt (e.g., $MnCl_2$), and levitated against gravity in a magnetic field gradient generated by two NdFeB magnets arranged with like poles facing each other (a MagLev device; Fig. 1; *SI Appendix*) (27, 28). Historically, MagLev, in air, of strongly diamagnetic materials (29) such as bismuth and pyrolytic graphite has been used to create devices such as a frictionless rotor (30), a tiltmeter–seismometer (31), and a pressure gauge (32). We and others have used MagLev in paramagnetic liquids for trapping small objects and separating diamagnetic materials on the basis of differences in density (28, 29, 33–47). This paper extends MagLev to the manipulation and orientation of objects of uniform density in 3D space. Nonspherical objects levitate with a well-defined orientation in the device. When the density of the object is uniform, the orientation that the levitating object adopts in the device depends only on the shape and aspect ratio of the object. We discovered a sharp, aspect-ratio-dependent transition in the orientation of objects

---

Significance

We describe several noncontact methods of orienting objects in three-dimensional (3D) space using Magnetic Levitation (MagLev), and report the discovery of a sharp geometry-dependent transition of the orientation of levitating objects. An analytical theory of the orientation of arbitrary objects in MagLev explains this transition. MagLev is capable of manipulating and orienting hard and soft objects, and objects of irregular shape. Because controlling the orientation of objects in space is a prerequisite for assembling complex structures from simpler components, this paper extends MagLev into 3D self-assembly, robotic assembly, and noncontact (stiction-free) orientation of hard and soft objects for applications in biomimetics, soft robotics, and stimulus-responsive materials, among others.
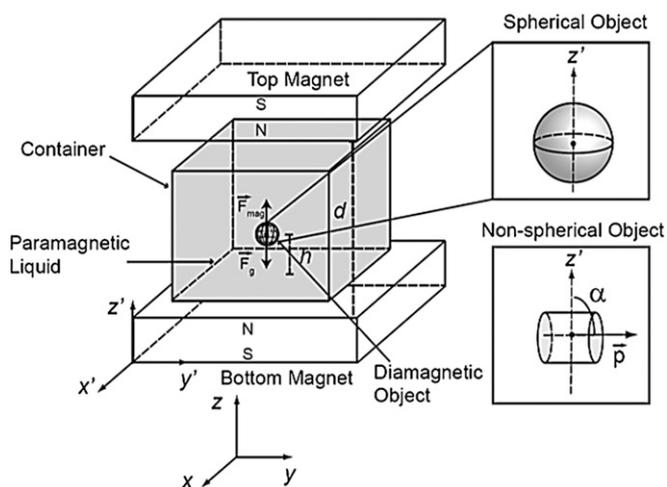
Fig. 1. Scheme describing MagLev. Two permanent magnets with like poles facing are arranged coaxially a distance d apart (the MagLev device). The laboratory fixed axes are x, y, and z, and the axes fixed on the MagLev device are x', y', and z'. A diamagnetic object (shown as a sphere) in a container containing paramagnetic liquid (dark gray) experiences a gravitational force $\vec{F}_g$ and a magnetic force $\vec{F}_{mag}$ when placed in the MagLev device. The schematic depicts the direction of the forces for an object of a higher density than the paramagnetic liquid. The direction of the vectors will be opposite for an object that is less dense than the liquid. When the two forces are in balance, the object levitates at a levitation height h. (*Inset*) A homogeneous spherical object has no unique plane of symmetry. To classify the orientation of nonspherical objects in the MagLev device (a cylinder is depicted here as an example), we define a unit vector $\vec{p}$ (direction vector), taken typically to be along the long axis of the object. The angle subtended by $\vec{p}$ and the z' axis (magnetic field axis) is α. (See *SI Appendix*.)

levitating in the MagLev device. We present an analytical theory that explains this transition and predicts the orientation of objects in the MagLev device.

The orientation of levitating objects in space can be manipulated in two ways: (*i*) by rotating and/or translating the MagLev device (with the objects suspended between the magnets), (*ii*) by keeping the MagLev device stationary while perturbing the magnetic field externally (e.g., by moving a small magnet or ferromagnetic probe close to the levitating objects).

Results and Discussion

The Orientations of Nonspherical Objects Levitating in a MagLev Device.

As a preliminary study, we levitated a Nylon screw (9 mm in length) in the MagLev device. Finite element simulations based on the parameters (dimensions, strength of the magnetic field, magnetic susceptibility of the solution) of this device show that, to a good approximation, the gradient of the magnetic field is linear, with a constant slope between the surface of the top magnet to the surface of the bottom magnet, and the magnetic field is zero at the center of the device (27). We rested the MagLev device on a flat laboratory bench, and hence the x'-, y'-, z' axes coincided with the x-, y-, z axes of the laboratory frame of reference. The concentration of $MnCl_2$ was 1.50 M, yielding a solution of density $\rho_s \sim 1.15$ g/cm^3 (measured with a pycnometer). The density of the solution was similar to that of the screw, $\rho_o = 1.15$ g/cm^3 (manufacturer's data). We chose the direction vector $\vec{p}$ to point along the long axis of the screw. The screw levitated at the center of the device and adopted an orientation with $\vec{p}$ parallel to the surface of the magnets (Fig. 2*A*). We next modified the shape of the screw by cutting the shaft to a length of 2.5 mm. The shortened screw, while still levitating at the center of the device, adopted an orientation with $\vec{p}$ pointing perpendicular to the surface of the magnets (Fig. 2*B*). Because we only changed the geometry of the screw, albeit substantially, we inferred that geometry played a role in determining the orientation of objects in this MagLev device.

We designed a series of experiments with model objects to explore the role of geometry for orientation in the MagLev device. We machined objects out of organic polymers with circular, annular, square, and triangular 2D cross-sections, each with a constant "characteristic" length, l. Depending on the object, l was the diameter of the circle, the outer diameter of the annulus, the side width of the square, or the length of the sides of the equilateral triangle (Fig. 2 *C–F*). We varied the thickness T of the objects in the third dimension to produce cylinders, annular
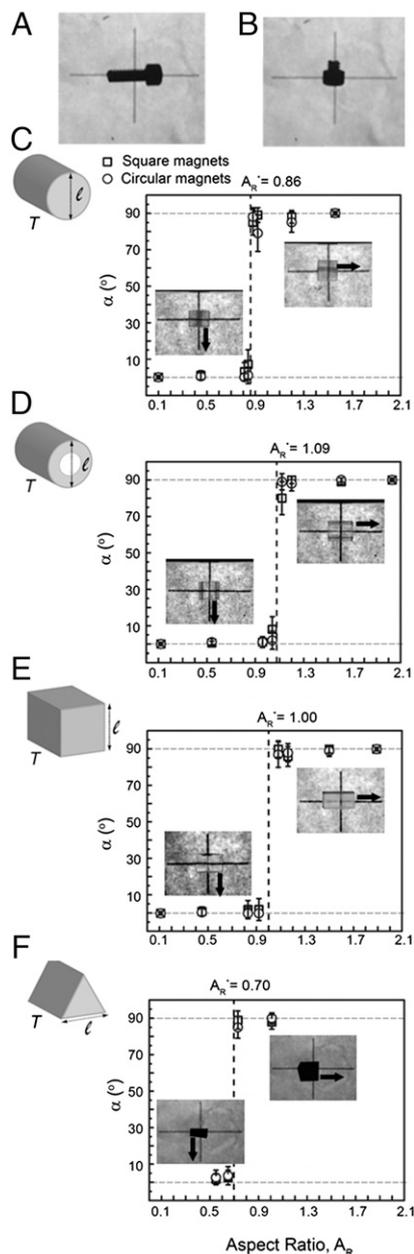

Fig. 2. Equilibrium orientations of nonspherical objects in MagLev. (*A* and *B*) A Nylon screw orients differently when the length of the shaft was reduced from 9.5 to 2.5 mm. (*C–F*) Plots of the orientation of the objects (angle α) versus their aspect ratios $A_R = T/l$ (schematic). Each data point is an average of seven replicate objects. The error bars represent the SD. The x-error bars are smaller than the data point. The dashed vertical line is the value of the critical aspect ratio A_R^*, predicted by theory. (*Insets*) Representative images of objects levitating in the MagLev device in each plot. The black arrow indicates the direction of $\vec{p}$. The cross in the background is for reference, and the horizontal line in the cross measured 30 mm.

cylinders, square prisms, and triangular prisms. Levitating these relatively simple, symmetric 3D objects with MagLev allowed us to obtain a theoretical understanding of the governing physics. To classify the shapes, we defined a nondimensional aspect ratio parameter A_R to be the ratio between the thickness of the object and its characteristic length (i.e., $A_R = T/l$; Fig. 2). We set $\vec{p}$ to be aligned along the thickness axis of the object.

We started by levitating objects of small A_R, and progressively levitated objects with larger A_R. We captured images of the objects along the y'–z' plane and measured the angle α that $\vec{p}$ subtended with respect to the z' axis of the device. We defined α to be zero when $\vec{p}$ was parallel to the z' axis. The value of α was clustered either around 0° or 90°—$\vec{p}$ was parallel or perpendicular to the surface of the magnets—with at most a 10° (typically <5°) variation observed between replicate objects. Plots of α versus A_R for each of the shapes revealed that α jumped abruptly from 0° to 90° at what appeared to be a critical value of A_R, which we denote as A_R^*. The value of A_R^* appeared to be different for the different shapes. For the cylinder we observed $0.84 \le A_R^* \le 0.88$, for the annular cylinder we observed $1.04 \le A_R^* \le 1.12$, for the square prism we observed $0.90 \le A_R^* \le 1.10$, and for the triangular prism we observed $0.65 \le A_R^* \le 0.73$. The value of A_R^* and the orientation of the objects in the y'–z' plane did not depend on the shape of the magnets, the levitation height of the objects (Fig. S1), or the distance d between the two magnets (varied from 45 to 65 mm) (Fig. S2), suggesting that the observed effects are purely a function of the shape of the objects.

The orientation of the object in the x'–y' plane, as expected, did depend on the shape of the magnets. For square magnets, the objects centered in the magnetic field and aligned along the diagonals (Fig. S3). For disk-shaped magnets, the final orientation of the object in the x'–y' plane was dependent on the history of sample. Shaking the container, or removing the container and replacing it in the MagLev device, caused the orientation of the object in this plane to change (data not shown). The orientation of the object in the y'–z' plane, however, was still fixed and determined only by A_R.

Modeling the Height and Orientation of Nonspherical Objects in MagLev.

The dependence of the height and orientation of objects on shape was one for which we wished to have an analytical treatment. We consider the potential energy of an arbitrary object located in a region with superimposed magnetic and gravitational fields (a MagLev system). Eq. 1 gives the energy density (energy per unit volume) of the MagLev system.

$$u = u_{mag} + u_{grav} = -\frac{1}{2\mu_o}\Delta\chi(\vec{r})\vec{B}^2 - \Delta\rho(\vec{r})\vec{g}\cdot\vec{h}. \quad \text{[1]}$$

In this equation, u_{mag} is the magnetic contribution and u_{grav} is the gravitational contribution to the total potential energy density, $\Delta\chi(\vec{r}) = \chi_o(\vec{r}) - \chi_s$ is the magnetic susceptibility of the object relative to a homogeneous medium, $\Delta\rho(\vec{r}) = \rho_o(\vec{r}) - \rho_s$ is the density of the object relative to a homogeneous medium, and $\vec{h} = (0, 0, h)$ is the height of the object. In general, the object can be heterogeneous in both density and magnetic susceptibility such that these functions depend on the position coordinate $\vec{r}$.

At static equilibrium, the potential energy $U = \int_V u\, dV$, where V is the volume of the object, has to be minimized. Finding the equilibrium configuration involves minimizing simultaneously the energy associated with the levitation height and orientation of the object. Parameterizing the object, and numerically solving the resulting set of multivariable equations (minimization has to be performed over the spatial coordinates and the distributions of density and susceptibility), provides the levitation height and equilibrium orientation for arbitrary objects in arbitrary magnetic fields.

Simplifications of Eq. 1 allow analytical closed-form solutions that provide physical insight. The equilibrium levitation height h_0 will occur where $dU/dh = 0$. For a linearly varying magnetic field, the levitation height of the centroid of the object in the MagLev

depends only on the average susceptibility $\bar{\chi}_o = 1/V\int_V\chi_o(\vec{r})dV$ and the average density $\bar{\rho}_o = 1/V\int_V\rho_o(\vec{r})dV$ of the object, regardless of the shape and the distribution of the heterogeneities within the object.

The equilibrium orientation(s) at angle α will occur at the local minima of U, where $dU/d\alpha = 0$ and $d^2U/d\alpha^2 > 0$. We choose a body-fixed coordinate system $\vec{p}(x'', y'', z'')$ aligned with the principal axes of the object, and fix the x'' axis to remain parallel to the x' axis of the MagLev reference frame (we include the full derivation and a procedure to find this preferred reference frame in *SI Appendix*). We proceed to analyze the rotation of the object around the x' axis with the same convention as in the experiments and parameterize orientation as the angle α that $\vec{p}$ subtends with respect to the z' axis. Eq. 2 gives this energy for an object that is homogeneous in susceptibility and density.

$$U(\alpha) = \beta\Delta\chi V\lambda_z^2(1-R)\sin^2\alpha. \quad \text{[2]}$$

In this equation, $\beta = 2B_0^2/\mu_0 d^2$, λ_z^2 is the principal second moment of area along the z'' axis, and R is the ratio of the principal second moments of area along the y''- and z'' axes.

Fig. 3A shows a plot of Eq. 2 at representative values of R. For values of $R < 1$, $U(\alpha) \propto \sin^2\alpha$, and the potential minima occur at $\alpha = 0°$ and 180°. For values of $R > 1$, $U(\alpha) \propto -\sin^2\alpha \propto \cos^2\alpha$, and the potential minima occur at $\alpha = 90°$ and 270°. All other values of α result in energies that lie within these extrema and are not stable. Thus, objects with uniform density will only orient with $\alpha = 0°$ or $\alpha = 90°$. This result rationalizes the experimental observations in Fig. 2. When R approaches 1, the linear theory predicts a flat energy landscape. Adapting the analysis that led to Eq. 2 for nonlinear magnetic fields by retaining higher order terms in the expression for $\vec{B}$ provides solutions for the orientation of these objects (*SI Appendix*).

We calculate the value of A_R^* at which it is energetically favorable for the objects to switch orientation from $\alpha = 0°$ or $\alpha = 90°$, and plot the results in Fig. 2 C–F as a dashed line (see *SI Appendix* for full calculation). Our calculations match our experimental results excellently. Furthermore, plotting α versus R results in the collapse of our data for all of the shapes onto a master curve where the transition between orientations occurs at $R = 1$ (Fig. 3B).

Manipulating the Orientation of Objects by Rotating the MagLev Device.

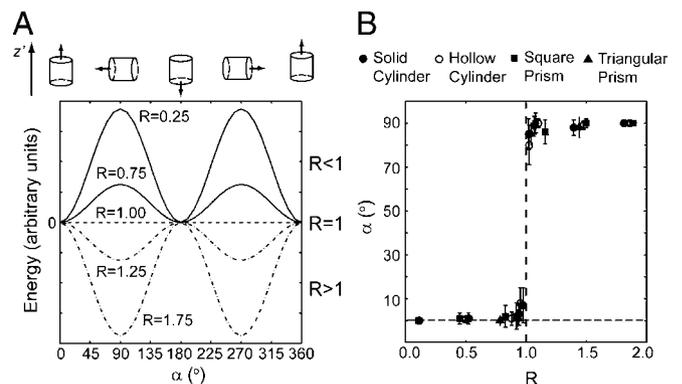We used a Nylon screw (8.5 mm in length) to illustrate the

Fig. 3. Energy and orientation of objects in MagLev. (*A*) Plot of the potential energy as a function of α (the angle that $\vec{p}$ makes with respect to the z' axis) (Eq. 2). R is the ratio of the second moment of area of the object. For $R < 1$, continuous black line, the two (degenerate) minima in potential energy occur at $\alpha = 90°$ and 270°. For $R > 1$, dashed and dotted black line, the two (degenerate) minima in potential energy occur at $\alpha = 0°$ and 180°. When R approaches 1, the linear theory predicts a flat energy landscape. The schematic at the top of the plot shows the orientation of the object with respect to z'. (*B*) Plot of α versus R for the experimental objects in Fig. 2. All of the data collapse onto a master curve with the transition in orientation at $R = 1$.

process involved in manipulating—without contact with a solid surface—the orientation of an object suspended inside an entirely closed container of paramagnetic liquid. We controlled the orientation of the screw by rotating the MagLev device together with the container of paramagnetic liquid. The concentration of $MnCl_2$ was again 1.50 M, and thus the screw levitated at the center of the device. Fig. 4 shows the orientation of the screw in the y–z plane when the device was rotated 360° counterclockwise about the x axis (the z' axis rotated relative to the z axis). For reference, we used a 30 × 22-mm cross as a background, keeping the cross fixed with respect to the laboratory frame of reference. The screw, suspended in solution, rotated in the laboratory frame of reference and tracked the angle of rotation of the magnets (Fig. 4B). Rotations about the other two axes resulted in similar outcomes (data not shown). We conclude that rotating (and translating) about the x-, y-, and z axes allows arbitrary orienting and positioning of objects in 3D with respect to the laboratory frame of reference. Fig. S4 demonstrates that the orientation of the objects can also be manipulated by moving only the magnets, while keeping the container stationary—a procedure that might be useful in certain situations: for example, when access to the oriented objects from the top of the container is desired.

Choosing a solution that has the same density as the object is important for contactless manipulation of objects by rotating the device. Fig. 4C shows the results when the density of the solution is lower than the density of the object (e.g., the same screw used

in Fig. 4B). Rotating the device to 45° caused the screw to translate toward the walls of the container, and eventually to contact the wall. Further rotation of the device to 90° caused the screw, which was touching the container, to flip, and prevented its further manipulation. Although not shown here, it is rational to speculate that normal forces on an object, due to contact with a hard wall, might damage or deform soft, sticky, or fragile objects.

Why does using a solution of lower density cause the screw to contact the wall of the container? When the density of the solution is equal to the density of the object, the gravitational force acting on the object is zero, and the center of volume of the object levitates at the center of the device (SI Appendix). When the density of the solution is less than that of the object, force balance requires that the object equilibrate at a smaller levitation height (the example shown in Fig. 4C), due to the nonzero gravitational force. Reversing the direction of the force vectors describes the situation for objects with a density higher than the solution, and the object equilibrates at a larger levitation height. Rotating the direction of the magnetic force (always acting along the z' axis) with respect to the direction of the gravitational force (always acting along the z axis) produces a component of the net force that acts perpendicular to the z axis. The perpendicular component of the force, which increases in magnitude with increasing angles of rotation and reaches a maximum at $\theta = 90°$, causes the object to translate toward the wall to maintain static equilibrium.

It is clear that when the gravitational force is zero, the object remains fixed at the center of the device. This configuration allows arbitrary rotations of the device without the object contacting the walls of the container. A practical means of matching the density of the liquid to an object of unknown density is to start with a concentrated solution of paramagnetic salt and progressively dilute the solution until the object levitates at the center of the device.
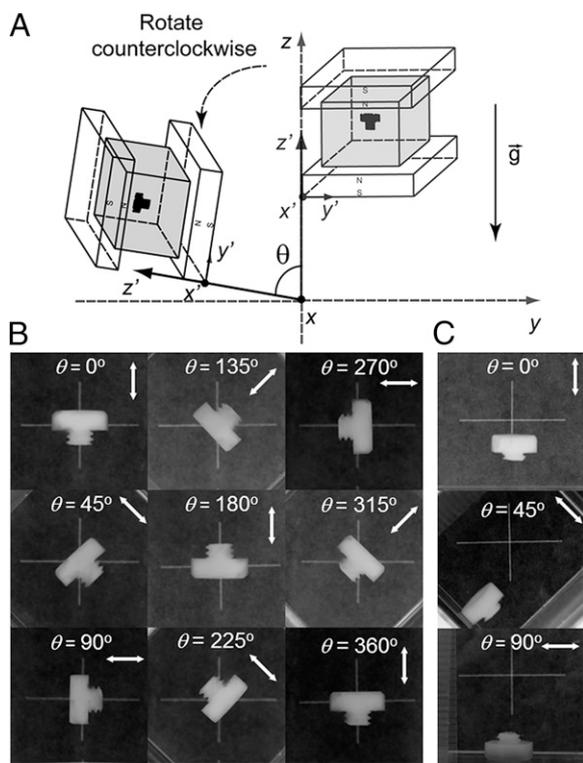
Manipulating the Orientation of Objects with External Magnets.
Another method of controlling the orientation of objects, without contact with a solid surface, is by using external magnets to modify the magnetic field generated by the fixed coaxial magnets in the MagLev device. It is energetically favorable for the paramagnetic liquid in the container to respond to changes in the magnetic field by redistributing volume to occupy regions of locally high field strength. This movement of liquid will indirectly cause the displacement of levitating diamagnetic objects in the MagLev device.

We demonstrate this method by manipulating the orientation of a Nylon screw (2 cm in length) in the x'–y' plane of a MagLev device equipped with disk-shaped magnets (Fig. 5). We used circular magnets because this geometry resulted in a circularly symmetric field in the x'–y' plane. Thus, the screw does not have any preferred orientation in this plane. Magnets with shapes of lower symmetry, for example square and rectangular magnets, favor the orientation of the object along specific planes of symmetry, such as along the diagonals (Fig. S4) (27, 47). Fig. 5B shows an image of the screw viewed along the x'–y' plane of the device. A cross pattern affixed to the bottom magnet is provided as a guide to the eye.

We used a small cubic magnet (0.64 × 0.64 × 0.64 cm, magnetic field strength at the surface ~0.4 T) to generate, externally, a localized region of high magnetic field strength to manipulate the orientation of the head of the screw. We brought the small magnet to a distance of about 2 cm from the head of the levitating screw (the walls of the container prevented a closer approach of the magnet). The head moved away from the small magnet and came to rest after rotating ~45° away from the surface of the external magnet. By moving the magnet around the exterior of the container, we oriented the head of the screw along the four principal axes of the cross (Fig. 5C). At each position, the screw remained at its new orientation even after the small magnet was moved away from the device. Furthermore, combinations of several external magnets allowed finer control of the orientation of levitating objects (Fig. S5).

Orienting Soft and Sticky Objects in MagLev.
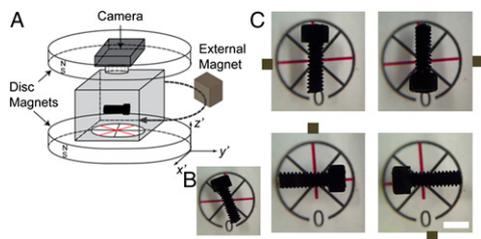MagLev shows particular promise for manipulating and controlling the orientation of

Fig. 4. Controlling the orientation of a levitating object in laboratory space by rotating the MagLev device. (A) Schematic of the experimental setup. θ is the angle that the z' axis makes relative to the z axis. (B) Experimental images taken along the y–z plane of a Nylon screw (8.5 mm in length) in the MagLev. We kept the cross in the background fixed relative to the laboratory. The screw tracks the position of the magnets, rotating a full 360° with respect to the laboratory frame of reference. The white double-headed arrows indicate the orientation of the axis of the magnetic field gradient. (C) Similar rotations caused the screw to translate and contact the wall of the container when the density of the screw was greater than the density of the solution. Further rotations caused the screw to flip orientation. For scale, the horizontal line in the cross is 30 mm.

Fig. 5. Manipulating the orientation of an object in the x'–y' plane of a MagLev device with an external magnet. (A) Schematic of the experimental setup. Due to the cylindrical symmetry of the magnetic field, the long axis of the screw does not have a preferred orientation in the x'–y' plane. The image in B shows one of the orientations the screw adopts when placed in the device. (C) We moved an external magnet close to the screw to align the screw head along the red lines of the pattern. The brown square indicates the approximate position of the external magnet. Scale bar, 5 mm. Also see Fig. S5 for images taken along the z'–y' plane of a screw being manipulated with external magnets.

soft materials. As proof or principle, we used MagLev to manipulate objects fabricated out of hydrogels, elastomers, and colloids—three classes of materials with diverse technological applications.

Hydrogels have been used to fabricate actuators (15), soft robots (5, 9), and artificial tissues (6–8). For example, directed assembly of hydrogel strips and blocks laden with different cell types is a promising method for engineering artificial tissues (6–8). Hydrogels used in biomimetic applications are soft (6–8), and tend to stick to surfaces due to the capillary action of the liquid film on the hydrogel surfaces. In Fig. 6A, we used MagLev in combination with an external magnet to orient a slab of poly (N-isopropylacrylamide) hydrogel; ordinarily, this material would deform or break when handled by a hard gripper (Young's modulus, E, of the hydrogel ~ 1,000 Pa). We inserted the object into the MagLev device by gently releasing the hydrogel from the mold into the paramagnetic liquid. In the MagLev container, the object was able to assume its natural shape, and the competing magnetic and gravitational forces acting on it determined its orientation. An external magnet allowed the control of the orientation of the sharp end of the hydrogel relative to the four principal axes of the cross.

In Fig. 6B, we controlled the orientation of a pneumatically actuated soft gripper made out of the silicone elastomer EcoFlex. The gripper, a modular part of a larger soft robot assembly (48), deforms easily when subject to moderate forces and tends to adhere to surfaces due to the low surface energy of cured Eco-Flex. Rotating the magnets allowed control over the orientation of the gripping face with respect to the laboratory frame of reference. We envision that MagLev, with further development, could extend modular strategies for the assembly (48) of robots to materials that are softer than elastomers [e.g., hydrogels (9)].

Self-assembled granular and colloidal materials, held together by relatively weak physical bonds, are a class of soft or fragile condensed matter that shows promise as stimuli-responsive materials and containers (11, 13, 14, 49–51). These materials, despite being composed predominantly of fluid, can adopt nonspherical shapes (i.e., they can demonstrate solid-like properties) due to the jamming of the colloidal particles on their surfaces (12, 51, 52). The capillary bonds that confer their solid-like properties are weak, and hence these solids have yield strengths on the order of $\gamma/R \sim$ tens of Pa (53). The surface tension of the liquid is γ (N/m), and the radius of the object is R. Although such low yield strengths are sufficient to maintain the shape of the objects against gravity and thermal agitation, once fabricated, these objects cannot be manipulated with hard grippers without causing irreversible plastic deformation due to localized shear melting of the jammed colloidal monolayer (53, 54). Fig. 6C shows control over the orientation of a nonspherical perfluorodecalin droplet covered with a jammed monolayer of 10-μm-diameter polystyrene particles. We

obtained the stable nonspherical peanut-like object by forcing two spherical particle-covered droplets to fuse by squeezing them mechanically. MagLev thus allows active manipulation of self-assembled diamagnetic granular structures without requiring the use of magnetic or paramagnetic particles (11). All of the manipulations demonstrated here can also be performed on composite objects with metallic components (Fig. S6).

Conclusion

Previous works have shown that an object placed in a MagLev device orients reliably based on the distribution of density in the object (47). In this paper, we have demonstrated experimentally and theoretically that, for objects with a homogeneous density, the distribution of volume (i.e., shape) also plays a relevant role in determining the orientation of the object. As a result, we have shown that MagLev provides a method to control the orientation of objects (including objects that are soft or fragile) in 3D without contact. The MagLev-based method for controlling the orientation of objects has a number of useful features. (i) It is non-damaging to fragile objects because it does not involve mechanical contact. (ii) It can flexibly orient objects of various shapes and a range of sizes. (iii) It can control the orientation of objects in 3D. (iv) It can control the orientation of objects inside an entirely closed container. (v) It is inexpensive. (vi) It can be made biocompatible with the use of chelated paramagnetic salts (45). (vii) Nonaqueous paramagnetic liquids (46) make it possible to use this method on moisture- or water-sensitive objects.

In its present form, this method also has several limitations. (i) MagLev, as we describe it here, operates best with materials with densities of $\sim 1 < \rho < 3$ g/cm^3. It is well-adapted to organic polymers, but less so to metals and heavier ceramics, although
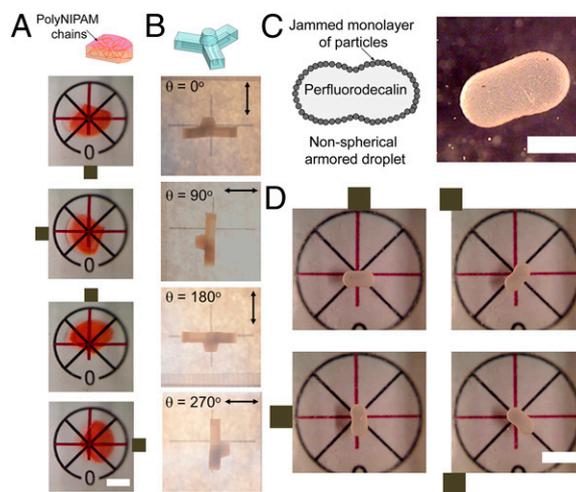

Fig. 6. Manipulation of soft, sticky, and easily deformable objects. (A) Photographs along the x'–y' plane showing control of the orientation of a poly(N-isopropylacrylamide) hydrogel using external magnets. We used the same experimental setup as in Fig. 4. The sharp end of the hydrogel was made to point in the four principal axes of the cross pattern. The brown square indicates the approximate position of the external magnet. The hydrogel levitated stably in each position after we withdrew the external magnet. (B) Images along the z'–y' plane of a soft-gripper component made out of EcoFlex 0030. The orientation of the gripping face was changed with respect to the laboratory frame of reference by rotating the magnets. The black double-headed arrows indicate the orientation of the axis of the magnetic field gradient, and θ is the angle of rotation of the magnets with respect to the z axis. (C) Schematic and picture of an armored droplet. The droplet adopts a stable peanut shape due to the jamming of the polystyrene particles on its interface. (D) We controlled the orientation of the armored droplet with respect to the cross pattern by using an external magnet. The manipulation of the position of the object with MagLev did not deform this soft solid. Scale bars: (A) 5 mm, (B) the horizontal line of the cross is 30 mm, (C) 2 mm, and (D) 5 mm.

with higher field strengths and more dense paramagnetic liquids, it should also apply to more dense objects. (*ii*) MagLev does not enable control over the orientation of objects smaller than ~10 μm in diameter because the magnetic and gravitational forces acting on these objects are insufficient to overcome Brownian motion, for the configuration and type of magnets used in this study.

These limitations aside, MagLev is compatible with a number of practical objects, such as plastic screws, polymeric objects, metal–polymer composites, soft hydrogels, elastomers, and granular matter. As such, we expect that further development of the MagLev as a strategy for orientation and assembly of components will ultimately prove useful in fields that require the manipulation and self-assembly of soft materials [e.g., components of soft robots (5, 9) or mechanically fragile components].

Materials and Methods

For the experiment shown in Fig. 4, we rotated the MagLev device with the container containing the screw anticlockwise about the *x* axis. For the experiment shown in Fig. 5, we levitated a black Nylon screw in a MagLev device equipped with disk-shaped magnets. A webcam glued to the top magnet imaged the position of the screw. A cross-hatch pattern glued to the bottom magnet served as a guide to the eye. Full experimental details are provided in *SI Appendix*.

1. Horn BKP, Ikeuchi K (1984) The mechanical manipulation of randomly oriented parts. *Sci Am* 251(2):100–111.
2. Cappelleri DJ, Cheng P, Fink J, Gavrea B, Kumar V (2011) Automated assembly for mesoscale parts. *IEEE Trans Autom Sci Eng* 8(3):598–613.
3. Schraft RD, Ledermann T (2003) Intelligent picking of chaotically stored objects. *Assem. Autom* 23(1):38–42.
4. Shea K, Ertelt C, Gmeiner T, Ameri F (2010) Design-to-fabrication automation for the cognitive machine shop. *Adv Eng Inform* 24(3):251–268.
5. Fusco S, et al. (2014) An integrated microrobotic platform for on-demand, targeted therapeutic interventions. *Adv Mater* 26(6):952–957.
6. Gurkan UA, Tasoglu S, Kavaz D, Demirel MC, Demirci U (2012) Emerging technologies for assembly of microscale hydrogels. *Adv Healthc Mater* 1(2):149–158.
7. Tasoglu S, et al. (2013) Paramagnetic levitational assembly of hydrogels. *Adv Mater* 25(8):1137–1143, 1081.
8. Du Y, Lo E, Ali S, Khademhosseini A (2008) Directed assembly of cell-laden microgels for fabrication of 3D tissue constructs. *Proc Natl Acad Sci USA* 105(28): 9522–9527.
9. Nawroth JC, et al. (2012) A tissue-engineered jellyfish with biomimetic propulsion. *Nat Biotechnol* 30(8):792–797.
10. Xia YN, Gates B, Yin YD, Lu Y (2000) Monodispersed colloidal spheres: Old materials with new applications. *Adv Mater* 12(10):693–713.
11. Dommersnes P, et al. (2013) Active structuring of colloidal armour on liquid drops. *Nat Commun* 4:2066.
12. Subramaniam AB, Abkarian M, Mahadevan L, Stone HA (2005) Colloid science: Nonspherical bubbles. *Nature* 438(7070):930.
13. Lee D, Weitz DA (2009) Nonspherical colloidosomes with multiple compartments from double emulsions. *Small* 5(17):1932–1935.
14. Shepherd RF, et al. (2006) Microfluidic assembly of homogeneous and Janus colloid-filled hydrogel granules. *Langmuir* 22(21):8618–8622.
15. Keplinger C, et al. (2013) Stretchable, transparent, ionic conductors. *Science* 341(6149): 984–987.
16. Murphy RJ (1982) US Patent 4,310,964 A.
17. Riley FJ (1996) *Assembly Automation: A Management Handbook* (Industrial Press, New York), 2nd Ed.
18. Agrawal A, Sun Y, Barnwell J, Raskar R (2010) Vision-guided robot system for picking objects by casting shadows. *Int J Robot Res* 29(2-3):155–173.
19. Buss M, Hashimoto H, Moore JB (1996) Dextrous hand grasping force optimization. *IEEE Trans Robot Autom* 12(3):406–418.
20. Yoshikawa T, Nagai K (1991) Manipulating and grasping forces in manipulation by multifingered robot hands. *IEEE Trans Robot Autom* 7(1):67–77.
21. Ilievski F, Mazzeo AD, Shepherd RF, Chen X, Whitesides GM (2011) Soft robotics for chemists. *Angew Chem Int Ed Engl* 50(8):1890–1895.
22. Martinez RV, et al. (2013) Robotic tentacles with three-dimensional mobility based on flexible elastomers. *Adv Mater* 25(2):205–212.
23. Brown E, et al. (2010) Universal robotic gripper based on the jamming of granular material. *Proc Natl Acad Sci USA* 107(44):18809–18814.
24. Bogue R (2012) Robots in the laboratory: A review of applications. *Ind Rob* 39(2): 113–119.
25. Pham DT, Yeo SH (1991) Strategies for gripper design and selection in robotic assembly. *Int J Prod Res* 29(2):303–316.
26. Bi ZM, Lang SYT, Shen W, Wang L (2008) Reconfigurable manufacturing systems: The state of the art. *Int J Prod Res* 46(4):967–992.
27. Mirica KA, Shevkoplyas SS, Phillips ST, Gupta M, Whitesides GM (2009) Measuring densities of solids and liquids using magnetic levitation: Fundamentals. *J Am Chem Soc* 131(29):10049–10058.
28. Kimura T, Mamada S, Yamato M (2000) Separation of solid polymers by magneto-Archimedes levitation. *Chem Lett* (11):1294–1295.
29. Catherall AT, Lopez-Alcaraz P, Benedict KA, King PJ, Eaves L (2005) Cryogenically enhanced magneto-Archimedes levitation. *New J Phys* 7:118.
30. Waldron RD (1966) Diamagnetic levitation using pyrolytic graphite. *Rev Sci Instrum* 37(1):29–35.
31. Simon I, Emslie AG, Strong PF, McConnel RK (1968) Sensitive tiltmeter utilizing a diamagnetic suspension. *Rev Sci Instrum* 39(11):1666–1671.
32. Evrard R, Boutry GA (1969) An absolute micromanometer using diamagnetic levitation. *J Vac Sci Technol* 6(2):279.
33. Beaugnon E, Tournier R (1991) Levitation of organic materials. *Nature* 349(6309):470.
34. Guevorkian K, Valles JM, Jr (2006) Swimming Paramecium in magnetically simulated enhanced, reduced, and inverted gravity environments. *Proc Natl Acad Sci USA* 103(35):13051–13056.
35. Hirota N, et al. (2004) Magneto-Archimedes separation and its application to the separation of biological materials. *Physica B* 346:267–271.
36. Ikezoe Y, Hirota N, Nakagawa J, Kitazawa K (1998) Making water levitate. *Nature* 393(6687):749–750.
37. Ikezoe Y, et al. (2002) Separation of feeble magnetic particles with magneto-Archimedes levitation. *Energy Convers Manage* 43(3):417–425.
38. Kimura T (2003) Study on the effect of magnetic fields on polymeric materials and its application. *Polym J* 35(11):823–843.
39. Lyuksyutov IF, Lyuksyutova A, Naugle DG, Rathnayaka KDD (2003) Trapping microparticles with strongly inhomogeneous magnetic fields. *Mod Phys Lett B* 17(17):935–940.
40. Lyuksyutov IF, Naugle DG, Rathnayaka KDD (2004) On-chip manipulation of levitated femtodroplets. *Appl Phys Lett* 85(10):1817–1819.
41. Mirica KA, Phillips ST, Shevkoplyas SS, Whitesides GM (2008) Using magnetic levitation to distinguish atomic-level differences in chemical composition of polymers, and to monitor chemical reactions on solid supports. *J Am Chem Soc* 130(52):17678–17680.
42. Valles JM, Jr, Lin K, Denegre JM, Mowry KL (1997) Stable magnetic field gradient levitation of Xenopus laevis: Toward low-gravity simulation. *Biophys J* 73(2):1130–1133.
43. Winkleman A, et al. (2007) Density-based diamagnetic separation: Devices for detecting binding events and for collecting unlabeled diamagnetic particles in paramagnetic solutions. *Anal Chem* 79(17):6542–6550.
44. Yokoyama K, Hirota N, Iwasaka M (2007) Separation of collagen by magneto-Archimedes levitation. *IEEE Trans Appl Supercond* 17(2):2181–2184.
45. Winkleman A, et al. (2004) A magnetic trap for living cells suspended in a paramagnetic buffer. *Appl Phys Lett* 85(12):2411–2413.
46. Bwambok DK, et al. (2013) Paramagnetic ionic liquids for measurements of density using magnetic levitation. *Anal Chem* 85(17):8442–8447.
47. Mirica KA, Ilievski F, Ellerbee AK, Shevkoplyas SS, Whitesides GM (2011) Using magnetic levitation for three dimensional self-assembly. *Adv Mater* 23(36):4134–4140.
48. Kwok SW, et al. (2013) Magnetic assembly of soft robots with hard components. *Adv Funct Mater* 24:2180–2187.
49. Cayre OJ, et al. (2012) pH-responsive colloidosomes and their use for controlling release. *Soft Matter* 8(17):4717–4724.
50. Dinsmore AD, et al. (2002) Colloidosomes: Selectively permeable capsules composed of colloidal particles. *Science* 298(5595):1006–1009.
51. Herzig EM, White KA, Schofield AB, Poon WCK, Clegg PS (2007) Bicontinuous emulsions stabilized solely by colloidal particles. *Nat Mater* 6(12):966–971.
52. Pieranski P (1980) Two-dimensional interfacial colloidal crystals. *Phys Rev Lett* 45(7): 569–572.
53. Subramaniam AB, Abkarian M, Mahadevan L, Stone HA (2006) Mechanics of interfacial composite materials. *Langmuir* 22(24):10204–10208.
54. Datta SS, Shum HC, Weitz DA (2010) Controlled buckling and crumpling of nanoparticle-coated droplets. *Langmuir* 26(24):18612–18616.

APPLIED PHYSICAL SCIENCES